European Journal of Medicinal Chemistry 101 (2015) 681–691

Contents lists available at ScienceDirect

European Journal of Medicinal Chemistry

journal homepage: http://www.elsevier.com/locate/ejmech

Research paper

Structure-kinetics relationships of Capadenoson derivatives as adenosine A_1 receptor agonists

Julien Louvel*, Dong Guo, Marjolein Soethoudt, Tamara A.M. Mocking, Eelke B. Lenselink, Thea Mulder-Krieger, Laura H. Heitman, Adriaan P. IJzerman

Division of Medicinal Chemistry, Leiden Academic Centre for Drug Research, Leiden University, P.O. Box 9502, 2300 RA Leiden, The Netherlands

ARTICLE INFO

Article history:
Received 11 February 2015
Received in revised form
10 July 2015
Accepted 11 July 2015
Available online 15 July 2015

Keywords:
Residence time
Structure-affinity relationships
Structure-kinetics relationships
Adenosine A_1 receptor
Extracellular loops

ABSTRACT

We report the synthesis and biological evaluation of new derivatives of Capadenoson, a former drug candidate that was previously advanced to phase IIa clinical trials. 19 of the 20 ligands show an affinity below 100 nM at the human adenosine A_1 receptor (hA_1AR) and display a wide range of residence times at this target (from approx. 5 min (compound **10**) up to 132 min (compound **5**)). Structure-affinity and structure-kinetics relationships were established, and computational studies of a homology model of the hA_1AR revealed crucial interactions for both the affinity and dissociation kinetics of this family of ligands. These results were also combined with global metrics (Ligand Efficiency, cLogP), showing the importance of binding kinetics as an additional way to better select a drug candidate amongst seemingly similar leads.

1. Introduction

The adenosine receptors (A_1, A_{2A}, A_{2B} and A_3), all of which accept adenosine as an endogenous ligand, belong to the G protein-coupled receptor superfamily of cell membrane-bound proteins (GPCRs). Their physiological and clinical relevance have been extensively studied [1]. Since the early 1990s, many synthetic ligands that selectively bind to a determined number of receptor subtypes have been developed, along with different functional profiles: partial or full agonists and antagonists/inverse agonists. Among these, compounds such as Capadenoson (Bayer) have emerged as non-ribose agonists for the A_1 Adenosine Receptor (A_1AR) and the $A_{2B}AR$ [2,3]. In the meantime, Otsuka Pharmaceuticals described a series of 4-amino-6-aryl-5-cyano-2-thiopyrimidines as selective agonists for the $A_{2A}AR$ [4]. Using this scaffold, our group has recently reported a series of derivatives that are selective for the A_1AR. 5 These compounds are shown in Fig. 1. In the latter paper we emphasized the relationships between the structure and binding kinetics of the new compounds. Indeed it has been shown 23 that dissociation kinetics, embodied by residence time (RT), may be a more accurate reflection of *in vivo* behavior than *in vitro* affinity and/or potency [6–8]. RT is defined as the reciprocal of the ligand's dissociation rate constant ($RT = 1/k_{off}$) and represents the lifetime of the ligand-receptor complex [9]. Incidentally, Capadenoson was advanced to clinical studies, but failed to show heart rate reduction in patients with atrial fibrillation in phase IIa clinical trials [10].

In the current study we report the synthesis and evaluation of 6-amino-4-aryl-3,5-dicyano-2-thiopyridines as (selective) A_1AR agonists. These compounds are derivatives of Capadenoson. They

Abbreviations: ADA, adenosine deaminase; Ac, acetyl; BCA, bicinchoninic acid; BEDROC, *Boltzmann-enhanced discrimination of receiver-operating characteristic*; BSA, bovine serum albumin; CPA, N^6-cyclopentyladenosine; CHO, Chinese hamster ovary; DMF, *N,N*-dimethylformamide; DMSO, dimethylsulfoxide; DPCPX, 1,3-dipropyl-8-cyclopentyl-xanthine; DTT, dithiothreitol; EC_{50}, concentration of unlabeled ligand which elicits 50% of the maximum response (E_{max}) in a functional assay at membranes of CHO cells stably expressing the adenosine A_1 receptor; EDTA, ethylenediaminetetraacetic acid; EF, Enrichment factor; E_{max}, maximum response elicited by an unlabeled ligand in a functional assay (relatively to CPA) at membranes of CHO cells stably expressing the adenosine A_1 receptor; FBS, fetal bovine serum; G418, Geneticin; GDP, guanosine diphosphate; GF, glass filter; GTP, guanosine triphosphate; GTPγS, guanosine 5′-O-[γ-thio]triphosphate; HPLC, high-pressure liquid chromatography; IC_{50}, concentration of unlabeled ligand which displaces 50% of [^{3}H]DPCPX binding to membranes of CHO cells stably expressing the adenosine A_1 receptor; K_i, affinity of ligand; k_{off}, dissociation rate constant at the hA_1AR; k_{on}, association rate constant at the hA_1AR; KRI, kinetic rate index; NMM, *N*-methylmorpholine; NMR, nuclear magnetic resonance; PBS, phosphate buffered saline; RT, residence time; SAR, structure-affinity relationships; SKR, structure kinetics relationships; THF, tetrahydrofuran; TLC, thin layer chromatography; Tris, tris(hydroxymethyl)aminomethane.

* Corresponding author.
E-mail address: j.a.louvel@lacdr.leidenuniv.nl (J. Louvel).

http://dx.doi.org/10.1016/j.ejmech.2015.07.023
0223-5234/

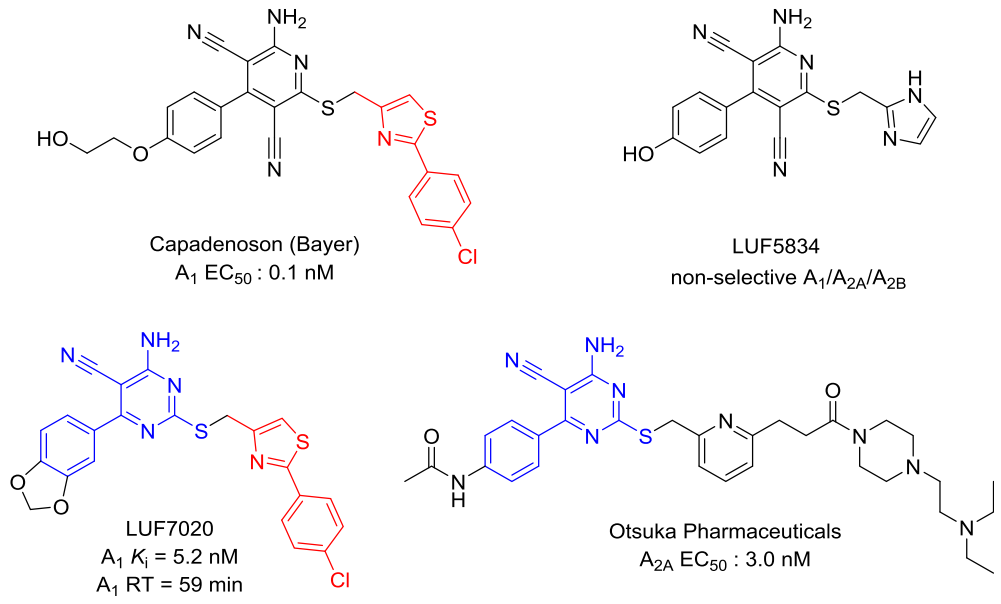

Fig. 1. Examples of non-ribose agonists for A_1AR (top and bottom left), A_1AR/A_{2A}AR/A_{2B}AR (top right), A_{2A}AR (bottom right).

were evaluated in radioligand displacement binding assays and in a competition association assay. The compounds are selective over the other AR subtypes and show high affinities and a broad range of kinetic profiles at the hA_1AR, and their Structure-Kinetics Relationships (SKR) were established. Their binding mode was analyzed in a homology model of hA_1AR, potentially shedding light on key structural features of the receptor that are involved in ligand dissociation. A representative set of ligands was also characterized in a functional assay, in which they emerged as A_1 receptor partial or full agonists.

2. Results and discussion

2.1. Design and synthesis

The *S*-substituted thiopyridines were synthesized in a two-step procedure. First, thiopyridines **1**–**3** were obtained in a previously reported one-pot, two-step reaction between malononitrile, thiophenol and various substituted benzaldehydes in the presence of piperidine and triethylamine at the reflux of ethanol, followed by displacement of thiophenolate by sodium sulfide at 80 °C in DMF [3]. Then the alkylation of the obtained thiols **1**–**3** with various alkyl chlorides in the presence of $NaHCO_3$ or DBU at r.t. in DMF afforded compounds **5**–**23** (Scheme 1) [3a,11]. Capadenoson **4** was synthesized using a reported procedure [11].

The alkyl chlorides **29**–**31** and **33**, **34** that were not commercially available were synthesized according to the method described previously [5], or by chlorination or bromination of 4-(chloromethyl)-2-(4-chlorophenyl)thiazole **32** (Scheme 1) [12].

2.2. Biology

All the compounds were tested in a radioligand displacement assay on the adenosine A_1 receptor in the presence of 2.5 nM [^{3}H]DPCPX [13]. All compounds, except **9**, displayed a high affinity for the human A_1AR (Ki < 100 nM). Subsequently, compounds with high A_1AR affinity were screened in a dual-point competition association assay in the presence of [^{3}H]DPCPX (RT = 4.8 min), which we recently applied to similar studies [5,14]. In brief, we determined specific [^{3}H]DPCPX binding in the presence of an unlabeled compound of interest at two time points and calculated the kinetic rate index (KRI), as defined by the ratio of bindings at the earlier and later time points, respectively; a KRI value above 1.0 indicates a slower dissociation from the target, while a value below 1.0 predicts a faster dissociation rate, as compared to the dissociation rate of the radioligand. Subsequently to this screening, the compounds with a KRI above 1.4 (Capadenoson had a KRI value of 1.42) were then subjected to a full competition association assay so as to quantitatively determine their kinetic parameters (k_{on}, k_{off}) and thus their RT.

2.2.1. Structure-affinity relationships and structure-kinetics relationships

All binding and kinetic data at the A_1AR discussed in this section are gathered in Table 1.

2.2.1.1. Aromatic substituent. Starting from Capadenoson, a brief screening of the substituent attached to the distal phenyl ring was carried out.

2.2.1.1.1. Structure-affinity relationships. In our hands, **4** (Capadenoson) had a high affinity (1.4 nM) at the A_1AR. Truncation of the terminal hydroxyethoxy fragment to a methoxy group led to a slightly decreased affinity (**5**, 5 nM). This result is different from our previous findings on a series of cyanopyrimidine analogs, for which a methoxy substituent at this position had led to a drastic drop in affinity (K_i < 100 nM) [5]. Further shortening of the chain to a hydroxy substituent did not affect binding (**6**, 1.5 nM). Finally, introducing a 3,4-methylenedioxy substituent, which had proven valuable in the previous study [5], yielded a similar affinity, comparable to that of **5** (**7**, 4.6 nM).

2.2.1.1.2. Structure-kinetics relationships. All four compounds displayed a KRI value above 1.4, **4** having the lower (1.42). **6** and **7** had similar KRI values (2.07 and 2.00, respectively), with associated residence times of 36 and 63 min respectively. The big difference between the residence times with identical KRI values can be explained by a big spread in the KRI value of **6** (values of 1.6 and 2.6). Noteworthy is that these three compounds (4, **6** and **7**) have longer residence times at the A_1AR than their cyanopyrimidine

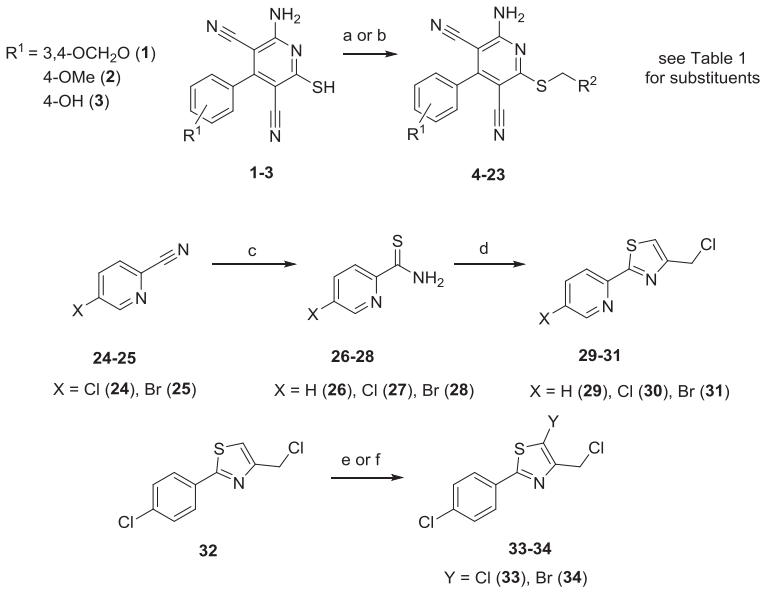

[a]Reagents and conditions : (a) R^2CH_2Cl, $NaHCO_3$, DMF, r.t, 26–100%; (b) R^2CH_2Cl, DBU, DMF, r.t, 78%. (c) $(NH_4)_2S$, Et_3N, pyridine, 50 °C, 48–57%; (d) 1,3-dichloroacetone, toluene, reflux, 40–70%; (e) HCl/HNO_3 4/3, Ac_2O, r.t., 84%; (f) Br_2, Ac_2O, r.t., 87%.

Scheme 1. Synthesis of Compounds 4–22 and alkylating agents 29–31 and 33–34.[a]

counterparts [5], which indicates a crucial influence of the additional cyano substituent on dissociation rates. **5** showed the highest KRI value (2.55), along with the longest residence time of the whole series of compounds in our study (132 min). Taken all together, the compounds with a more lipophilic substituent (**5** and **7**) show slower dissociation from the A_1AR than the compounds bearing a hydroxyl group (**4** and **6**). As far as association rates are concerned, **4** displays the highest value ($k_{on} = 2.4 \times 10^7$ M^{-1} min^{-1}), six to ten times higher than **5** ($k_{on} = 2.6 \times 10^6$ M^{-1} min^{-1}), **6** ($k_{on} = 4.3 \times 10^6$ M^{-1} min^{-1}) and **7** ($k_{on} = 2.4 \times 10^6$ M^{-1} min^{-1}).

2.2.1.2. Thiazole substituent. With the 4-methoxy substituent on the phenyl ring adjacent to the pyridine core the influence of the nature of the substituents on the thiazole ring was then studied.

2.2.1.2.1. 5-Position. Two compounds bearing a halogen atom (**8**, Cl and **9**, Br) on the 5-position of the thiazole ring were synthesized to study the potential for halogen bonding at this position [15]. Introduction of a chloro substituent led to an 18-fold decrease in affinity (**8**, 88 nM *vs* **5**, 5 nM), while a bromo substituent further halved the affinity (**9**, 162 nM). The latter compound was not evaluated in the competition association assay because it displayed an affinity above the 100 nM threshold. **8**, on the other hand, had a KRI of 1.79, with an associated residence time of 36 min. Both affinity and RT show that no halogen bonding seems to be taking place, because both the affinity and the residence time decrease from **5** to **8**.

2.2.1.2.2. 2-Position

2.2.1.2.2.1. Structure-affinity relationships. The unsubstituted thiazole ($R^3 = H$) gave a high affinity (**10**, 1.3 nM), the highest of this subseries of compounds. Addition of a phenyl ring led to a significant decrease in affinity (**11**, 8.4 nM), albeit still in the nanomolar range. When the phenyl ring was exchanged for a morpholine ring, a higher affinity was measured (**12**, 3.2 nM). These results seem to be in contrast with our previous findings on the cyanopyrimidine analogs of these compounds, for which the affinity decreased in the morpholino < phenyl < H order [5]. This could be due to the presence of an additional cyano substituent on the central heterocycle, and/or the methoxy group instead of a methylenedioxy group on the distal phenyl ring, both of which could slightly change the binding pose of the ligand.

The substitution pattern of the phenyl ring was then studied. The introduction of a halogen on the 4-position did not lead to a significant increase in affinity (4-F, **13**, 5.0 nM *vs* H, **11**, 8.4 nM). An increase in size and lipophilicity in the halogen series also led to similar results (F, **11**; Cl, **5**; Br, **14**; I, **15**). In contrast to the analogous cyanopyrimidines, moving the chloro substituent along the ring did not change the affinity much (4-Cl, **5**, 5.0 nM; 3-Cl, **16**, 12 nM; 2-Cl, **17**, 11 nM), which seems to indicate that the dihedral angle between the thiazolyl and phenyl rings does not have a small value (which would be disfavored by the presence of a 2-chloro substituent) [16] in the binding pose. Also, dichlorination on the 3 and 4 position gave a similar affinity (**18**, 11 nM), which is again in contrast with our previous findings on cyanopyrimidine analogs. Replacing the chloro substituent with a methoxy group did not change the affinity (**19**, 9.3 nM), while the introduction of a lipophilic methyl group led to a twofold loss of binding (**20**, 19 nM).

Finally, the phenyl ring was changed into a 2-pyridyl ring: the introduction of a nitrogen atom at this position with a halogen substituent at the *para* position (relative to the thiazole) leads to an increase of the sigma-hole on the halogen atom, which could reinforce halogen bonding with residues in the vicinity of the ligand [15]. The effect of the pyridyl ring itself was negligible in terms of affinity (**21**, 9.5 nM *vs* **11**, 8.4 nM). Addition of a chlorine or a bromine atom led to a 5- and 14-fold decrease when compared to

Table 1
Structure—affinity relationships and Structure-Kinetics relationships of 4–23.

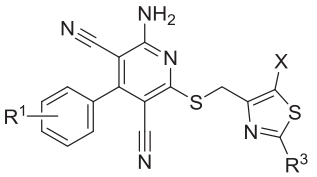

nr.	R^1	R^3	X	K_i (nM) ± SEM[a]	KRI[b]	k_{on} (M^{-1} min^{-1})[d]	k_{off} (min^{-1})[e] (RT (min))[f]
4	4-O$(CH_2)_2$OH	4-Cl-Ph	H	1.4 ± 0.15	1.42 (1.29; 1.55)	2.4 ± 0.90 × 10^7	0.036 ± 0.013 (27.8)
5	4-OMe	4-Cl-Ph	H	5.0 ± 0.57	2.55 (1.56; 3.54)	2.6 ± 0.6 × 10^6	0.0076 ± 0.0003 (132)
6	4-OH	4-Cl-Ph	H	1.5 ± 0.47	2.07 (1.58; 2.56)	4.3 ± 1.6 × 10^6	0.028 ± 0.01 (35.7)
7	3,4-OCH_2O	4-Cl-Ph	H	4.6 ± 1.1	2.00 (1.90; 2.20)	2.4 ± 0.25 × 10^6	0.016 ± 0.001 (62.5)
8	4-OMe	4-Cl-Ph	Cl	88 ± 8	1.79 (1.72; 1.86)	1.4 ± 0.26 × 10^6	0.028 ± 0.002 (35.7)
9	4-OMe	4-Cl-Ph	Br	162 ± 14	–[c]	–[c]	–[c]
10	4-OMe	H	H	1.3 ± 0.38	1.00 (0.97; 1.03)	–[c]	–[c]
11	4-OMe	Ph	H	8.4 ± 0.80	1.23 (1.16; 1.30)	–[c]	–[c]
12	4-OMe	morpholine	H	3.2 ± 1.2	1.12 (0.91; 1.33)	–[c]	–[c]
13	4-OMe	4-F-Ph	H	2.3 ± 0.21	1.56 (1.49; 1.63)	4.6 ± 0.90 × 10^6	0.033 ± 0.007 (30.3)
14	4-OMe	4-Br-Ph	H	3.8 ± 0.34	1.55 (1.51; 1.59)	2.4 ± 0.50 × 10^6	0.020 ± 0.005 (50.0)
15	4-OMe	4-I-Ph	H	3.9 ± 0.41	2.07 (1.83; 2.32)	1.6 ± 0.40 × 10^6	0.011 ± 0.004 (90.9)
16	4-OMe	3-Cl-Ph	H	12 ± 0.19	1.60 (1.32; 1.88)	7.7 ± 2.2 × 10^5	0.025 ± 0.007 (40.0)
17	4-OMe	2-Cl-Ph	H	11 ± 0.68	1.53 (1.32; 1.74)	9.4 ± 2.5 × 10^5	0.024 ± 0.007 (41.7)
18	4-OMe	3,4-diCl-Ph	H	11 ± 0.78	2.35 (2.23; 2.46)	1.1 ± 0.20 × 10^6	0.019 ± 0.005 (52.6)
19	4-OMe	4-OMe-Ph	H	9.3 ± 0.95	1.22 (1.19; 1.25)	–[c]	–[c]
20	4-OMe	4-Me-Ph	H	19 ± 2.7	1.25 (1.25; 1.26)	–[c]	–[c]
21	4-OMe	2-Pyr	H	9.5 ± 0.90	1.08 (1.11; 1.05)	–[c]	–[c]
22	4-OMe	5-Cl-2-Pyr	H	24 ± 4.3	1.64 (1.64; 1.64)	3.4 ± 0.28 × 10^6	0.035 ± 0.008 (28.6)
23	4-OMe	5-Br-2-Pyr	H	53 ± 8.6	1.71 (1.66; 1.75)	1.4 ± 0.20 × 10^6	0.030 ± 0.002 (33.3)

[a] K_i ± SEM (n = 3), obtained from radioligand binding assays with [^{3}H]DPCPX on CHO cell membranes stably expressing human adenosine A_1 receptors.
[b] KRI (n_1, n_2) ($n = 2$), obtained from dual-point competition association assays with [^{3}H]DPCPX on CHO cell membranes stably expressing human adenosine A_1 receptors.
[c] Not determined.
[d] k_{on} ± SEM (n ≥ 3), obtained from competition association assays with [^{3}H]DPCPX on CHO cell membranes stably expressing human adenosine A_1 receptors.
[e] k_{off} ± SEM (n ≥ 3), obtained from competition association assays with [^{3}H]DPCPX on CHO cell membranes stably expressing human adenosine A_1 receptors.
[f] RT (residence time) = $1/k_{off}$.

the phenyl-ring analogs, respectively (**22**, 24 nM and **23**, 53 nM). One explanation for the loss of affinity could be that the halogen substituent interacts with the binding pocket not through halogen bonding but lipophilic or dipolar interactions. As a result an increase of the size of the sigma-hole would diminish these interactions through local depletion of electron density on the chlorine atom.

2.2.1.2.2.2. Structure-kinetics relationships. The ligand with the shortest residence time was the smaller one (R^3 = H, **10**), with a KRI of 1.00. Adding a phenyl group slightly decreased the dissociation rate (**11**, KRI = 1.23), while introducing a morpholino substituent had virtually no effect (**12**, KRI = 1.12). Introduction of a halogen atom on the phenyl ring dramatically increased residence time at the A_1AR. Indeed, *para*-fluoro (**13**)-, chloro (**5**)-, bromo (**14**)- and iodo (**15**)-substituted compounds all displayed KRI values above 1.50, with associated residence times ranging from 30 min (**13**) to 132 min (**5**). Surprisingly, there does not seem to be any progression in the halogen series in terms of size, lipophilicity or electronegativity that would correlate with the evolution of residence time, since RT follows the F < Br < I < Cl order. When looking at association rates, however, there is a somewhat clearer trend following the increase of electronegativity or σ parameter. Indeed, the fluoro-substituted compound associates almost twice as fast as its chloro and bromo analogs, which in turn associate 1.5 times faster than the iodo compound. Moving the chloro substituent to the *meta* or *ortho* position has deleterious effects both on residence time and association rate constant; indeed, **16** and **17** both dissociate more

than 3 times faster and associate 30 times slower than **5**. Dichlorination at the *meta* and *para* positions led to a more than twofold decrease of residence time when compared to the *para*-chlorinated derivative (**18**, 53 min *vs* **5**, 132 min), but slightly longer than the *meta*-chlorinated compound (**16**, 40 min). The same trend was observed in terms of evolution of the association rate constant. Introduction of a methoxy or methyl group at the 4-position led to a greatly increased dissociation rate (**19**, KRI = 1.22; **20**, KRI = 1.25).

Changing the phenyl ring into a 2-pyridyl ring led to a shorter residence time in the case of the unsubstituted derivative (**21**, KRI = 1.08 *vs* **11**, KRI = 1.23), as well as for the compound with a chloro substituent *para* to the thiazole (**22**, RT = 29 min *vs* **5**, RT = 132 min). A slight decrease was observed in the case of the bromo derivative (**23**, RT = 33 min *vs* **14**, RT = 48 min).

2.2.2. Ligand efficiency and Lipophilicity [17]

Ligand Efficiency (LE) is one of the many metrics used in drug discovery for the selection of lead compounds; it represents the binding energy per (non-hydrogen) atom of a given compound to a target ($LE = \Delta G/N$, where DG is the Gibbs energy of binding and N the number of non-hydrogen atoms) [18]. The higher LE, the more efficient the binding, and the more likely it is to be a good drug candidate. Reference compound **4** has an LE of 0.35, making it a good drug candidate for this metric. From the other compounds in this study, most (16) were in the $0.32 \leq LE \leq 0.38$ range. Out of the remaining four, three had a ligand efficiency below 0.30 (**8**, **9** and **23**), and one above 0.4 (**10**, LE = 0.47). The compound with the longest residence time had the same ligand efficiency (**5**, LE = 0.35) as Capadenoson (**4**). Only its affinity was slightly lower than that of **4** (5.0 nM *vs* 1.4 nM). The calculated clogP of **4** is 5.04, whereas for **5** it is 5.73. In the end, this deviation from the 'rule of 5' [19] could be compensated by the significant gain in residence time. Also noteworthy is that the least lipophilic compound **10** (clogP = 3.10) is also the one with the shortest residence time; the opposite does not hold true, however, because the most lipophilic compound that was also screened for binding kinetics does not have the longest residence time (**8**, clogP = 6.50, RT = 36 min). For compounds with the same ligand efficiency as **5**, it appears that there are compounds which are more lipophilic, yet dissociate faster from the A_1AR (**14**, clogP = 5.89, RT = 50 min; **15**, clogP = 6.05, RT = 91 min). Hence, there is no obvious correlation between overall compound lipophilicity and residence time.

2.2.3. Selectivity

Six compounds representative of the structural variations introduced in the study, as well as showing a good affinity at the hA_1AR, were selected to be tested for their selectivity against the other adenosine receptor subtypes. All compounds were selective over the A_{2A}AR, showing negligible displacement of [^{3}H]ZM241385 [20], the reference radioligand for A_{2A}AR, at a concentration of 1 μM. At A_{2B}AR, compounds **11** and **10** showed modest to good affinity (63% displacement of the A_{2B}AR radioligand [^{3}H]PSB603 at 1 μM and $K_i = 23$ nM [21], respectively). This trend was the same as with the cyanopyrimidine analogs [5]. At the A_3AR, the displacement of the radioligand [^{3}H]PSB11 at 1 μM of the selected compounds stayed below 50% [22], indicating a selectivity of at least 100-fold for the A_1AR. The most selective compound across all subtypes was **4** (Table 2).

2.2.4. Functional assays

The same six compounds were tested in a [^{35}S]GTPγS functional assay. In our hands, **4** gave the response (E_{max} = 97%) of a full agonist (CPA [23], 100%), and so did **11**, **12** and **21**. Compounds **5** and **10** showed a lower E_{max} of 83% and 55%, respectively, which are characteristic of partial agonists (Table 2). All tested compounds showed EC_{50} values in the nanomolar range, between 1.1 nM for **4** and 7.6 nM for **21** (Table 2), indicating that these ligands are potent agonists at the hA_1AR.

2.3. Computational studies

Finally, we decided to further investigate the ligand-receptor interactions through docking studies. To this end, a homology model of the hA_1AR receptor was constructed (see Experimental details).

When looking at the docking pose of **5** (Fig. 2), it appears that this compound (and the others in this study) binds with the distal six-membered aromatic ring pointing inside the binding cavity, which is comparable to the binding mode of LUF5834 in the A_{2A} receptor [24]. The pyridine ring of **5** interacts with Phe171 (located on EL2) *via* a π−π interaction, which corresponds to the interaction of LUF5834 and Phe168 observed at the A_{2A} receptor. The interaction of Asn254 with the amino group and the vicinal nitrile (Asn253 in A_{2A}AR) *via* hydrogen bonding is similar too in the two receptor models.

For the distal nitrile group, however, an interaction occurs with Asn70, while in the A_{2A} receptor a bridging water molecule between Ala63 and Tyr9 plays this role [24]. Another residue, Lys265, located in EL3, also seems to entertain a crucial interaction with the ligands; it is involved in two hydrogen bonds, one with the nitrogen atom of the central pyridine ring of the ligand, and one with the nitrogen atom of the thiazole ring. The substituent borne by the thiazole ring (i.e. the substituted aromatic ring) does not appear to be involved in any specific interaction as far as the model can show, and the 4-chloro substituent appears to nest into the surface defined by the backbone of TM7 in the vicinity of Lys265. The rest of the aromatic system seems to be exposed to the solvent, since it is in the vicinity of Tyr271 which is forming a hydrogen bond with Asn70.

Table 2
Selectivity data and functional profile of selected compounds.

	Displ. at A_{2A}AR at 1 μM (%)[a]	Displ. at A_{2B}AR at 1 μM (%)[b]	Displ. at A_3AR at 1 μM (%)[c]	EC_{50} (nM)[d]	E_{max} (%)[e]
4	0.0 (−6.0, 3.0)	2.5 (5.0, 0.0)	1.2 (2.4, 0.0)	1.1 ± 0.80	97 ± 6.7
5	5.8 (7.6, 4.0)	20 (31, 8.5)	19 (21, 18)	2.9 ± 0.7	83 ± 3.7
10	0.0 (−10, 1.0)	23 ± 2	50 (46, 54)	1.5 ± 0.58	55 ± 4.1
11	0.0 (−7.0, −11)	63 (70, 55)	27 (22, 33)	1.9 ± 0.41	105 ± 9.8
12	0.0 (−17, −2.0)	0.0 (−15, 1.0)	51 (48, 54)	1.9 ± 0.51	104 ± 5.4
21	0.0 (−13, 1.0)	0.0 (−30, −38)	22 (15, 30)	7.6 ± 0.72	99 ± 2.6

[a] % displacement at 1 μM concentrations of specific [^{3}H]ZM241385 binding on HEK 293 cell membranes stably expressing human adenosine A_{2A} receptors.
[b] % displacement at 1 μM concentrations of specific [^{3}H]PSB603 binding on CHO cell membranes stably expressing human adenosine A_{2B} receptors or affinity (cpd **10**).
[c] % displacement at 1 μM concentrations of specific [^{3}H]PSB11 binding on CHO cell membranes stably expressing human adenosine A_3 receptors.
[d] Concentration causing half-maximal stimulation of specific binding of [^{35}S]GTPγS in CHO cell membranes expressing human adenosine A_1 receptors (n = 3).
[e] Maximum specific binding of [^{35}S]GTPγS in CHO cell membranes expressing human adenosine A_1 receptors, with 0% being the binding in the absence of any ligand (buffer) and 100% being the reference agonist CPA at a concentration of 100 μM (n = 3).

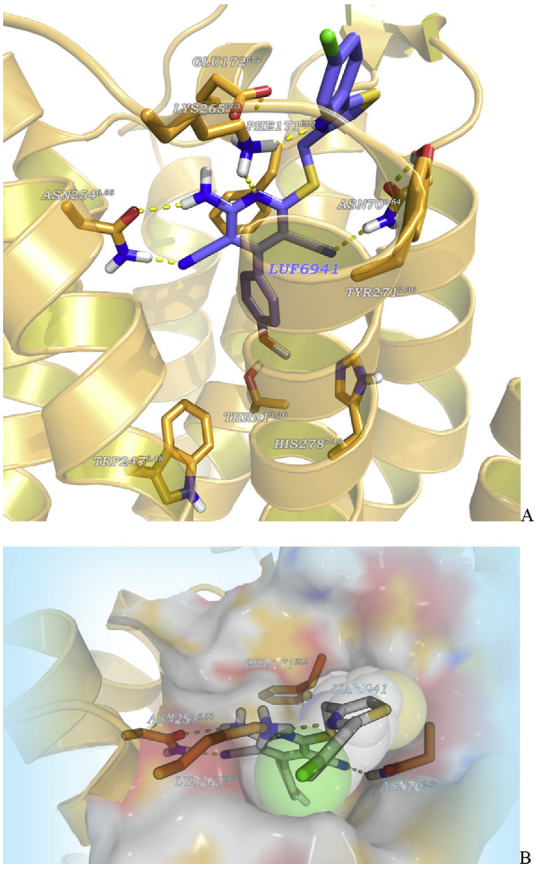

Fig. 2. Docking pose of **5** (LUF6941) in the homology model of hA1AR, showing hydrogen bonding interactions (yellow dashed lines) with the residues of the binding site. A: side view. B: top view, with molecular surfaces of both the ligand and the receptor; receptor surface color code: grey = hydrophobic, red = negatively charged, blue = positively charged; ligand atoms color code: white = carbon, blue = nitrogen, green = chlorine, yellow = sulfur, red = oxygen, white = hydrogen. (For interpretation of the references to color in this figure legend, the reader is referred to the web version of this article.)

Although homology modeling is speculative in nature, particularly for the extracellular loops of the receptor, a few hypotheses can be made using the abovementioned observations. The thiazole moiety seems to play a crucial role in binding to EL3 *via* Lys265, thereby anchoring EL3 in a specific conformation. Out of this interaction the formation of a cavity arises, in which the chloro substituent seems to fit best. The chlorine atom could then act as a "lipophilic cap", preventing the access of water molecules to the binding site and the hydrogen bonds [25], as illustrated by the slower dissociation rate displayed by **5**. This seems to be in agreement with the increased dissociation rate observed when the size of the σ-hole of the chlorine atom is increased, thereby allowing it to interact with water through halogen-bonding more readily [26]. Increasing the size of the halogen atom (to Br or I, compounds **14** or **15**) leads to a decrease in residence time, which could be due to the looser or less compact association between the ligand and the receptor in this region. When replacing the phenyl ring with a morpholino group (**12**), the exposed substituent may not be lipophilic enough to slow down dissociation, and the same would go in the absence of a substituent (**10**).

3. Conclusion

A series of derivatives of Capadenoson (including Capadenoson itself) were synthesized that display high affinity and selectivity at the hA_1AR. In addition to structure-affinity relationships, structure-kinetics relationships were established, and it was shown that the residence time of Capadenoson (**4**) can be increased from 28 min up to 132 min by replacing its 4-(2-hydroxyethoxy) substituent with a 4-methoxy substituent (**5**). The crucial importance of the substituent borne by the thiazole moiety was also highlighted, showing that a 4-halogen-bearing phenyl ring allowed for slower dissociation rates, whereas the use of more flexible and polar groups (**12**) led to shorter residence times. Furthermore, the docking pose of **5** in a homology model of hA_1AR revealed the potential importance of EL3 in receptor–ligand complex dissociation, suggesting the halogen substituent to act as a lipophilic cap. A selection of compounds was also characterized in a functional assay, showing partial to full (55–105%) activation of the hA_1AR. These results, taken together with the similar drug-like properties of **4** (LE = 0.35, cLogP = 5.04) and **5** (LE = 0.35, cLogP = 5.73), seem to indicate the importance of another hit selection criterion, namely residence time, in the early stages of drug discovery. Lack of efficacy in clinical studies, as was the case for **4** [10], might be linked to a shorter residence time for the target in case, whereas on-target toxicity may be associated with longer residence times [27]. Whether **5** would be a better lead candidate than **4** is an open question, but addressing the kinetics of the drug–receptor interaction provides room for a more detailed and educated hit and lead optimization process.

4. Experimental section

4.1. Chemistry

All solvents and reagents were purchased from commercial sources and were of analytical grade. Demineralised water is simply referred to as H_2O, as was used in all cases unless stated otherwise (i.e. brine). ^1H and ^{13}C NMR spectra were recorded on a Bruker AV 400 liquid spectrometer (^1H NMR, 400 MHz; ^{13}C NMR, 100 MHz) at ambient temperature. Chemical shifts are reported in parts per million (ppm), are designated by δ and are downfield to the internal standard tetramethylsilane (TMS) in $CDCl_3$. Coupling-constants are reported in Hz and are designated as J. Analytical purity of the final compounds was determined by high pressure liquid chromatography (HPLC) with a Phenomenex Gemini 3μ C18 110A column (50 × 4.6 mm, 3 μm), measuring UV absorbance at 254 nm. Sample preparation and HPLC method was – unless stated otherwise – as follows: 0.3–0.8 mg of compound was dissolved in 1 mL of a 1:1:1 mixture of $CH_3CN/H_2O/tBuOH$ and eluted from the column within 15 min, with a three component system of H_2O/CH_3CN/1% TFA in H_2O, decreasing polarity of the solvent mixture in time from 80/10/10 to 0/90/10. All compounds showed a single peak at the designated retention time and are at least 95% pure. Liquid chromatography–mass spectrometry (LC–MS) analyses were performed using Thermo Finnigan Surveyor – LCQ Advantage Max LC-MS system and a Gemini C18 Phenomenex column (50 × 4.6 mm, 3 μm). The sample preparation was the same as for HPLC analysis. The elution method was set up as follows: 1–4 min isocratic system of H_2O/CH_3CN/1% TFA in H_2O, 80:10:10, from the 4th min, a gradient was applied from 80:10:10 to 0:90:10 within 9 min, followed by 1 min of equilibration at 0:90:10 and 1 min at 80:10:10. Thin-layer chromatography (TLC) was routinely performed to monitor the progress of reactions, using aluminum coated Merck silica gel F254 plates. Purification by column chromatography was achieved by use of Grace Davison Davisil silica column material (LC60A 30–200 micron). Solutions were concentrated using a Heidolph laborota W8 2000 efficient rotary evaporation apparatus and by a high vacuum on a Binder APT line Vacuum Drying Oven. The procedure for a series of similar compounds is given as a

general procedure for all within that series, annotated by the numbers of the compounds. The procedure for the synthesis of similar compounds is given as a general procedure; deviations therefrom are given below for each compound.

4.2. General procedure to thioamides **27**–**28**

Benzonitriles **24**–**25** (1 eq.) were dissolved in pyridine (1.5 M), triethylamine (1.1 eq.) and ammoniumsulfide (1.1 eq.) were added and the mixture was heated to 50 °C. After completion of the reaction, the mixture was extracted three times with EtOAc, dried with $MgSO_4$, filtered and concentrated in vacuo.

4.3. 5-Chloropyridine-2-carbothioamide **27**

Prepared from 5-chloropicolinonitrile **24**, yield 57%. ^{1}H NMR (400 MHz, MeOD) δ 8.63 (d, J = 8.4 Hz, 1H), 8.55 (s, 1H), 7.95 (d, J = 8.8 Hz, 1H).

4.4. 5-Bromopyridine-2-carbothioamide **28**

Prepared from 5-bromopicolinonitrile **25**, yield 48%. ^{1}H NMR (400 MHz, MeOD) δ 8.63 (d, J = 8.4 Hz, 1H), 8.55 (s, 1H), 7.95 (d, J = 8.8 Hz, 1H).

4.5. General procedure to alkylating agents **29**–**31**

Pyridinecarbothioamides **26**–**28** (1 eq.) and dichloroacetone (1 eq.) were dissolved in toluene (1 M) and heated to reflux (110 °C). After completion of the reaction, the mixture was cooled to room temperature and extracted with EtOAc (3 times) and the organic layer was washed (brine), dried ($MgSO_4$), filtered and concentrated in vacuo. The product was purified by column chromatography.

4.6. 4-(Chloromethyl)-2-(pyridin-2-yl)thiazole **29**

Prepared from benzothioamide **26**. Eluent for column chromatography: (1% MeOH in CH_2Cl_2), yield 47%. ^{1}H NMR (400 MHz, $CDCl_3$) δ 8.61 (d, J = 4.4 Hz, 1H), 8.20 (d, J = 8.0 Hz, 1H), 7.80 (td, J = 7.8, 1.5 Hz, 1H), 7.42 (s, 1H), 7.35–7.32 (m, 1H), 4.76 (s, 2H).

4.7. 4-(Chloromethyl)-2-(5-chloropyridin-2-yl)thiazole **30**

Prepared from benzothioamide **27**. Eluent for column chromatography: (10% EtOAc in Pet Ether), yield 70%. ^{1}H NMR (400 MHz, $CDCl_3$) δ 8.55 (d, J = 2.0 Hz, 1H), 8.15 (d, J = 8.4 Hz, 1H), 7.78 (dd, J = 8.4, 2.4 Hz, 1H), 7.43 (s, 1H), 4.77 (s, 2H).

4.8. 4-(Chloromethyl)-2-(5-bromopyridin-2-yl)thiazole **31**

Prepared from benzothioamide **28**. Eluent for column chromatography: (10% EtOAc in Pet Ether), yield 40%. ^{1}H NMR (400 MHz, $CDCl_3$) δ 8.65 (d, J = 1.2 Hz, 1H), 8.09 (d, J = 8.4 Hz, 1H), 7.93 (dd, J = 8.4, 2.4 Hz, 1H), 7.43 (s, 1H), 4.75 (s, 2H).

4.9. 3-Chloro-4-(chloromethyl)-2-(4-chlorophenyl)thiazole **33**

To a solution of 4-(chloromethyl)-2-(4-chlorophenyl)thiazole **32** (244 mg, 1 mmol) in Ac_2O (35 mL) was added a mixture of concentrated HCl (0.48 mL) and HNO_3 (0.36 mL). After 1 h at room temperature, H_2O (200 mL) was added, the precipitate was filtered and washed with H_2O, and dried under vacuum to afford **33** as a solid (233 mg, 84%). ^{1}H NMR (400 MHz, $CDCl_3$) δ 7.81–7.78 (m, 2H), 7.43–7.41 (m, 2H), 4.71 (s, 2H).

4.10. 3-Bromo-4-(chloromethyl)-2-(4-chlorophenyl)thiazole **34**

To a solution of 4-(chloromethyl)-2-(4-chlorophenyl)thiazole **32** (244 mg, 1 mmol) in Ac_2O (35 mL) was added bromine (0.10 mL, 3 mmol). After 8 h at room temperature, H_2O (200 mL) was added, the precipitate was filtered and washed with H_2O, and dried under vacuum to afford **34** as a solid (282 mg, 87%). ^{1}H NMR (400 MHz, $CDCl_3$) δ 7.82–7.79 (m, 2H), 7.44–7.40 (m, 2H), 4.72 (s, 2H).

4.11. General procedure to final aminopyridines **5**–**23**

Central aminopyridines **1**–**3** (1 eq.), alkylating agents (1 eq.), and $NaHCO_3$ (1 eq.) were dissolved in DMF (1 mL) and stirred at rt. The work-up procedure after completion of the reaction is described for each compound independently.

4.12. 2-Amino-6-{[2-(4-chlorophenyl)thiazol-4-yl]methylthio}-4-(4-methoxyphenyl)pyridine-3,5-dicarbonitrile **5**

Prepared from central aminopyridine **2** and 4-(chloromethyl)-2-(4-chlorophenyl)thiazole. H_2O was added to the reaction mixture and the precipitate was filtered. The product was recrystallized from $CHCl_3$ and washed with EtOAc and MeOH over filter. Light beige solid (392 mg, 0.8 mmol, 53%). ^{1}H NMR (400 MHz, DMSO) δ 7.95–7.92 (m, 3H), 7.57–7.55 (m, 2H), 7.50–7.47 (m, 2H), 7.10 (d, J = 7.6 Hz, 2H), 4.63 (s, 2H), 3.83 (s, 3H). ^{13}C NMR (101 MHz, DMSO) δ 165.9, 165.7, 160.8, 159.7, 158.1, 152.5, 134.9, 131.7, 130.2, 129.4, 127.8, 125.8, 125.8, 118.9, 115.5, 114.1, 93.4, 85.9, 55.4, 29.3. HPLC t_R: 12.3 min.

4.13. 2-Amino-6-({[2-(4-chlorophenyl)thiazol-4-yl]methyl}thio)-4-(4-hydroxyphenyl)pyridine-3,5-dicarbonitrile **6**

Prepared from central aminopyridine **3** and 4-(chloromethyl)-2-(4-chlorophenyl)thiazole. H_2O was added to the reaction mixture, extracted three times with EtOAc, dried with $MgSO_4$, filtered and concentrated in vacuo. The product was purified by Preparative TLC (50%–100% EtOAc in PE). Light yellow solid (83 mg, 0.17 mmol, 34%). ^{1}H NMR (400 MHz, DMSO) δ 10.07 (s, 1H), 7.95–7.91 (m, 3H), 7.56 (d, J = 8.4 Hz, 2H), 7.36 (d, J = 8.4 Hz, 2H), 6.90 (d, J = 8.4 Hz, 2H), 4.63 (s, 2H). ^{13}C NMR (101 MHz, DMSO) δ 165.9, 165.7, 159.8, 159.5, 158.4, 152.5, 134.9, 131.7, 130.3, 129.3, 127.8, 124.1, 118.8, 115.6, 115.4, 93.3, 85.8, 29.3. HPLC t_R: 11.3 min.

4.14. 2-Amino-6-{[2-(3,4-methylenedioxyphenyl)thiazol-4-yl]methylthio}-4-(4-methoxyphenyl)pyridine-3,5-dicarbonitrile **7**

Prepared from central aminopyridine **1** and 4-(chloromethyl)-2-(4-chlorophenyl)thiazole. H_2O was added to the reaction mixture and the precipitate was filtered. Beige/yellow powder (50%). ^{1}H NMR (400 MHz, DMSO) δ 8.50–7.80 (m, 5H), 7.55 (d, J = 8.4 Hz, 2H), 7.13 (s, 1H), 7.08 (d, J = 8.0 Hz, 1H), 7.02 (d, J = 8.0 Hz, 1H), 6.13 (s, 2H), 4.62 (s, 2H). ^{13}C NMR (101 MHz, DMSO) δ 165.8, 165.7, 159.6, 158.0, 152.5, 149.0, 147.3, 134.9, 131.7, 129.4, 127.8, 127.3, 123.0, 118.9, 115.4, 109.0, 108.6, 101.8, 93.5, 86.1, 29.3. HPLC t_R: 11.2 min.

4.15. 2-Amino-6-({[5-chloro-2-(4-chlorophenyl)thiazol-4-yl]methyl}thio)-4-(4-methoxyphenyl)pyridine-3,5-dicarbonitrile **8**

Prepared from central aminopyridine **2** and **33**. H_2O was added to the reaction mixture and the precipitate was filtered. The product was washed with EtOAc and methyl *tert*-butyl ether. Yield 46%. ^{1}H NMR (400 MHz, DMSO) δ 8.00 (br s, 2H), 7.89 (d, J = 7.6 Hz, 2H), 7.57 (d, J = 7.6 Hz, 2H), 7.50 (d, J = 7.8 Hz, 2H), 7.10 (d, J = 7.8 Hz, 2H), 4.70 (s, 2H), 3.83 (s, 3H). ^{13}C NMR (101 MHz, DMSO) δ 165.5,

163.2, 160.9, 159.7, 158.1, 148.4, 135.6, 130.8, 130.2, 129.4, 127.6, 125.7, 122.9, 115.4, 114.1, 93.4, 86.2, 55.4, 26.8. HPLC t_R: 11.8 min. MS (ESI+) m/z = 523.93.

4.16. 2-Amino-6-({[5-bromo-2-(4-chlorophenyl)thiazol-4-yl] methyl}thio)-4-(4-methoxyphenyl)pyridine-3,5-dicarbonitrile ***9***

Prepared from central aminopyridine **2** and **34**. H_2O was added to the reaction mixture and the precipitate was filtered. The product was washed with EtOAc. Yield 91%. ^{1}H NMR (400 MHz, DMSO) δ 8.00 (br s, 2H), 7.89 (d, *J* = 7.2 Hz, 2H), 7.57 (d, *J* = 7.2 Hz, 2H), 7.50 (d, *J* = 7.5 Hz, 2H), 7.10 (d, *J* = 7.5 Hz, 2H), 4.69 (s, 2H), 3.83 (s, 3H). ^{13}C NMR (101 MHz, DMSO) δ 166.0, 165.6, 160.9, 159.7, 158.1, 150.8, 135.5, 130.8, 130.3, 129.4, 127.6, 125.7, 115.5, 115.4, 114.1, 107.7, 93.3, 86.2, 55.4, 28.0. HPLC t_R: 8.4 min (50–100% gradient of acetonitrile). MS (ESI+) m/z = 569.87.

4.17. 2-Amino-4-(4-methoxyphenyl)-6-(thiazol-4-ylmethylthio) pyridine-3,5-dicarbonitrile ***10***

Prepared from central aminopyridine **2** and 4-(chloromethyl)-thiazole hydrochloride, using 2 equivalents of $NaHCO_3$. Beige solid (154 mg, 0.41 mmol, 82%). ^{1}H NMR (400 MHz, DMSO) δ 9.07 (s, 1H), 7.86 (s, 1H), 7.48 (d, *J* = 8.8 Hz, 2H), 7.10 (d, *J* = 8.8 Hz, 2H), 4.63 (s, 2H), 3.84 (s, 3H). ^{13}C NMR (101 MHz, DMSO) δ 166.0, 160.8, 159.7, 158.1, 154.3, 151.9, 130.2, 125.8, 117.7, 115.4, 114.1, 93.3, 85.9, 55.3, 29.3. HPLC t_R: 9.8 min.

4.18. 2-Amino-4-(4-methoxyphenyl)-6-[(2-phenylthiazol-4-yl) methylthio]pyridine-3,5-dicarbonitrile ***11***

Prepared from central aminopyridine **2** and 4-(chloromethyl)-2-phenylthiazole. H_2O was added to the reaction mixture and the precipitate was filtered. Off-white/light brown solid (157 mg, 0.34 mmol, 68%). ^{1}H NMR (400 MHz, DMSO) δ 7.93–7.92 (m, 2H), 7.88 (s, 1H), 7.49 (t, *J* = 3.2 Hz, 5H), 7.10 (d, *J* = 8.8 Hz, 2H), 4.64 (s, 2H), 3.83 (s, 3H). ^{13}C NMR (101 MHz, DMSO) δ 167.0, 166.0, 160.8, 159.7, 158.1, 152.3, 132.8, 130.5, 130.3, 130.2, 129.3, 126.1, 125.8, 119.6, 118.3, 115.5, 114.1, 93.4, 85.9, 55.3, 29.3. HPLC t_R: 11.8 min.

4.19. 2-Amino-4-(4-methoxyphenyl)-6-[(2-morpholinothiazol-4-yl)methylthio]pyridine-3,5-dicarbonitrile ***12***

Central aminopyridine **2** (1 eq.), 4-(chloromethyl)-2-morpholinothiazole (1 eq.), and DBU (2 eq.) were dissolved in DMF (1 mL) and stirred at rt. After completion of the reaction, H_2O was added to the reaction mixture and the precipitate was filtered. Beige solid (181 mg, 0.39 mmol, 78%). ^{1}H NMR (400 MHz, DMSO) δ 7.48 (d, *J* = 8.8 Hz, 2H), 7.10 (d, *J* = 8.4 Hz, 2H), 6.97 (s, 1H), 4.36 (s, 2H), 3.83 (s, 3H), 3.69 (m, 4H), 3.35-3.34 (m, 4H). ^{13}C NMR (101 MHz, DMSO) δ 171.1, 166.3, 162.4, 160.9, 159.7, 158.1, 130.3, 125.9, 115.6, 114.1, 106.1, 93.4, 85.8, 65.4, 55.4, 48.1, 47.9, 30.0. HPLC t_R: 8.8 min.

4.20. 2-Amino-6-{[2-(4-fluorophenyl)thiazol-4-yl]methylthio}-4-(4-methoxyphenyl)pyridine-3,5-dicarbonitrile ***13***

Prepared from central aminopyridine **2** and 4-(chloromethyl)-2-(4-fluorophenyl)thiazole. H_2O was added to the reaction mixture and the precipitate was filtered. The product was washed with acetone over filter. Off-white powder (93 mg, 0.20 mmol, 40%).^{1}H NMR (400 MHz, DMSO) δ 7.99–7.96 (m, 2H), 7.87 (s, 1H), 7.48 (d, *J* = 8.4 Hz, 2H), 7.36–7.32 (m, 2H), 7.10 (d, *J* = 8.4 Hz, 2H), 4.63 (s, 2H), 3.83 (s, 3H). ^{13}C NMR (101 MHz, DMSO) δ 165.9, 160.8, 158.1, 152.3, 130.2, 128.5, 128.4, 125.8, 118.4, 116.4, 116.2, 115.5, 114.1, 55.4, 29.3. HPLC t_R: 11.7 min.

4.21. 2-Amino-6-{[2-(4-bromophenyl)thiazol-4-yl]methylthio}-4-(4-methoxyphenyl)pyridine-3,5-dicarbonitrile ***14***

Prepared from central aminopyridine **2** and 4-(chloromethyl)-2-(4-bromophenyl)thiazole. H_2O was added to the reaction mixture and the precipitate was filtered. The product was washed with EtOAc over filter. Light beige solid (182 mg, 0.34 mmol, 68%). ^{1}H NMR (400 MHz, DMSO) δ 7.91–7.86 (m, 3H), 7.69 (d, *J* = 6.8 Hz, 2H), 7.48 (d, *J* = 7.2 Hz, 2H), 7.10 (d, *J* = 7.2 Hz, 2H), 4.63 (s, 2H), 3.83 (s, 3H). ^{13}C NMR (101 MHz, DMSO) δ 165.9, 165.7, 160.8, 159.7, 158.1, 152.5, 132.2, 132.0, 128.0, 125.8, 123.6, 118.8, 115.5, 114.1, 93.4, 85.9, 55.3, 29.3. HPLC t_R: 12.6 min.

4.22. 2-Amino-6-{[2-(4-iodophenyl)thiazol-4-yl]methylthio}-4-(4-methoxyphenyl)pyridine-3,5-dicarbonitrile ***15***

Prepared from central aminopyridine **2** and 4-(chloromethyl)-2-(4-iodophenyl)thiazole. H_2O was added to the reaction mixture and the precipitate was filtered. The precipitate was washed with EtOAc over filter, filtrate was concentrated in vacuo, yielding the pure product as a light brown solid (177 mg, 0.30 mmol, 60%). ^{1}H NMR (400 MHz, DMSO) δ 7.90 (s, 1H), 7.87 (d, *J* = 8.4 Hz, 2H), 7.71 (d, *J* = 8.0 Hz, 2H), 7.48 (d, *J* = 8.8 Hz, 2H), 7.10 (d, *J* = 8.4 Hz, 2H), 4.63 (s, 2H), 3.83 (s, 3H). ^{13}C NMR (101 MHz, DMSO) δ 166.0, 165.9, 160.8, 159.7, 158.1, 152.5, 138.0, 132.3, 130.2, 127.9, 125.8, 20.0, 118.7, 115.5, 114.1, 97.1, 93.4, 85.9, 55.3, 29.3. HPLC t_R: 12.8 min.

4.23. 2-Amino-6-{[2-(3-chlorophenyl)thiazol-4-yl]methylthio}-4-(4-methoxyphenyl)pyridine-3,5-dicarbonitrile ***16***

Prepared from central aminopyridine **2** and 4-(chloromethyl)-2-(3-chlorophenyl)thiazole. H_2O was added to the reaction mixture and the precipitate was filtered. Beige/yellow powder (388 mg, 0.79 mmol, 100%). ^{1}H NMR (400 MHz, DMSO) δ 7.89 (s, 3H), 7.55–7.48 (m, 4H), 7.10 (d, *J* = 8.4 Hz, 2H), 4.64 (s, 2H), 3.83 (s, 3H). ^{13}C NMR (101 MHz, DMSO) δ 165.9, 160.9, 159.7, 152.6, 134.7, 134.0, 131.3, 130.2, 130.1, 125.8, 125.4, 124.9, 119.3, 115.5, 114.1, 93.4, 55.4, 29.2. HPLC t_R: 12.3 min.

4.24. 2-Amino-6-{[2-(2-chlorophenyl)thiazol-4-yl]methylthio}-4-(4-methoxyphenyl)pyridine-3,5-dicarbonitrile ***17***

Prepared from central aminopyridine **2** and 4-(chloromethyl)-2-(2-chlorophenyl)thiazole. H_2O was added to the reaction mixture and the precipitate was filtered. The product was purified by Preparative TLC (50% EtOAc in PE). Yellow solid (93 mg, 0.19 mmol, 38%). ^{1}H NMR (400 MHz, DMSO) δ 8.19–8.17 (m, 1H), 8.06 (s, 1H), 7.65–7.63 (m, 1H), 7.51–7.48 (m, 4H), 7.10 (d, *J* = 8.8 Hz, 2H), 4.67 (s, 2H), 3.83 (s, 3H). ^{13}C NMR (101 MHz, DMSO) δ 166.0, 162.2, 160.9, 159.8, 158.2, 151.3, 131.2, 131.0, 130.8, 130.7, 130.7, 130.3, 127.8, 125.8, 120.3, 115.5, 114.1, 93.4, 85.9, 55.4, 29.2. HPLC t_R: 12.1 min.

4.25. 2-Amino-6-{[2-(3,4-dichlorophenyl)thiazol-4-yl]methylthio}-4-(4-methoxyphenyl)pyridine-3,5-dicarbonitrile ***18***

Prepared from central aminopyridine **2** and 4-(chloromethyl)-2-(3,4-dichlorophenyl)thiazole. H_2O was added to the reaction mixture and the precipitate was filtered. Light beige solid (224 mg, 0.43 mmol, 86%). ^{1}H NMR (400 MHz, DMSO) δ 8.11 (s, 1H), 7.97 (s, 1H), 7.89 (d, *J* = 8.4 Hz, 1H), 7.75 (d, *J* = 8.4 Hz, 1H), 7.48 (d, *J* = 8.4 Hz, 2H), 7.10 (d, *J* = 8.8 Hz, 2H), 4.64 (s, 2H), 3.83 (s, 3H). ^{13}C NMR (101 MHz, DMSO) δ 165.8, 164.1, 160.8, 159.7, 158.1, 152.7, 133.2, 132.7, 132.1, 131.5, 130.2, 127.4, 126.2, 125.8, 119.7, 115.5, 114.1,

93.4, 85.9, 55.3, 29.2. HPLC t_R: 13.1 min.

4.26. 2-Amino-4-(4-methoxyphenyl)-6-{[2-(4-methoxyphenyl) thiazol-4-yl]methylthio}pyridine-3,5-dicarbonitrile **19**

Prepared from central aminopyridine **2** and 4-(chloromethyl)-2-(4-methoxyphenyl)thiazole. H_2O was added to the reaction mixture and the precipitate was filtered. Beige solid (100 mg, 0.39 mmol, 78%). ^{1}H NMR (400 MHz, DMSO) δ 7.86 (d, J = 8.4 Hz, 2H), 7.77 (s, 1H), 7.48 (d, J = 8.4 Hz, 2H), 7.10 (d, J = 8.4 Hz, 2H), 7.04 (d, J = 8.8 Hz, 2H), 4.61 (s, 2H), 3.83 (s, 3H), 3.82 (s, 3H). ^{13}C NMR (101 MHz, DMSO) δ 166.9, 166.0, 160.9, 160.8, 159.7, 158.1, 151.9, 130.2, 127.7, 125.8, 125.7, 117.2, 115.5, 114.6, 114.1, 93.4, 85.9, 55.4, 29.4. HPLC t_R: 11.7 min.

4.27. 2-Amino-4-(4-methoxyphenyl)-6-[(2-p-tolylthiazol-4-yl) methylthio]pyridine-3,5-dicarbonitrile **20**

Prepared from central aminopyridine **2** and 4-(chloromethyl)-2-(4-methylphenyl)thiazole. H_2O was added to the reaction mixture and the precipitate was filtered. The product was washed with EtOAc over filter. Off-white/light beige solid (98 mg, 0.21 mmol, 42%). ^{1}H NMR (400 MHz, DMSO) δ 7.83–7.80 (m, 3H), 7.48 (d, J = 8.0 Hz, 2H), 7.29 (d, J = 7.2 Hz, 2H), 7.10 (d, J = 8.0 Hz, 2H), 4.63 (s, 2H), 3.83 (s, 3H), 2.34 (s, 3H). ^{13}C NMR (101 MHz, DMSO) δ 167.1, 166.0, 160.8, 159.7, 158.1, 152.1, 140.2, 130.3, 130.2, 129.8, 126.0, 125.8, 119.0, 117.8, 115.5, 114.1, 93.4, 85.9, 55.3, 29.4, 20.9. HPLC t_R: 12.2 min.

4.28. 2-Amino-6-[(2-pyridinethiazol-4-yl)methylthio]-4-(4-methoxyphenyl)pyridine-3,5-dicarbonitrile **21**

Prepared from central aminopyridine **2** and **29**. H_2O was added to the reaction mixture and the precipitate was filtered. The product was triturated in CH_2Cl_2. Yield 26%. ^{1}H NMR (400 MHz, DMSO) δ 8.63 (s, 1H), 8.50–7.80 (br. s, 2H), 8.11 (d, J = 6.8 Hz, 2H), 7.97 (s, 2H), 7.50 (d, J = 3.2 Hz, 3H), 7.11 (d, J = 7.2 Hz, 2H), 4.66 (s, 2H), 3.84 (s, 3H). ^{13}C NMR (101 MHz, DMSO) δ 168.3, 165.9, 160.8, 159.7, 158.1, 152.7, 150.2, 149.7, 137.8, 130.2, 125.8, 125.2, 120.7, 119.2, 115.5, 114.1, 93.4, 85.9, 55.3, 29.4. HPLC t_R: 9.9 min. MS (ESI+) m/z = 457.13.

4.29. 2-Amino-6-{[2-(4-chloropyridine)thiazol-4-yl]methylthio}-4-(4-methoxyphenyl)pyridine-3,5-dicarbonitrile **22**

Prepared from central aminopyridine **2** and **30**. H_2O was added to the reaction mixture and the precipitate was filtered. The product was triturated in CH_2Cl_2. Yield 44%. ^{1}H NMR (400 MHz, DMSO) δ 8.69 (s, 1H), 8.60–7.75 (br s, 2H), 8.12 (d, J = 8.4 Hz, 1H), 8.08 (dd, J = 8.5, 1.3 Hz, 1H), 8.01 (s, 1H) 7.48 (d, J = 8.5 Hz, 2H), 7.10 (d, J = 8.5 Hz, 2H), 4.65 (s, 2H), 3.83 (s, 3H). ^{13}C NMR (101 MHz, DMSO) δ 166.8, 165.9, 160.8, 159.7, 158.1, 153.0, 148.7, 148.3, 137.5, 132.1, 130.2, 125.8, 121.2, 120.4, 115.5, 114.1, 93.4, 85.9, 55.3, 29.3. HPLC t_R: 10.8 min. MS (ESI+) m/z = 491.07.

4.30. 2-Amino-6-{[2-(4-bromopyridine)thiazol-4-yl]methylthio}-4-(4-methoxyphenyl)pyridine-3,5-dicarbonitrile **23**

Prepared from central aminopyridine **2** and **31**. H_2O was added to the reaction mixture and the precipitate was filtered. The product was triturated in CH_2Cl_2. Yield 63%. ^{1}H NMR (400 MHz, DMSO) δ 8.77 (s, 1H), 8.60–7.75 (br. s, 2H), 8.20 (d, J = 8.4 Hz, 1H), 8.03 (t, J = 9.6 Hz, 2H), 7.48 (d, J = 8.2 Hz, 2H), 7.10 (d, J = 8.3 Hz, 2H), 4.65 (s, 2H), 3.83 (s, 3H). ^{13}C NMR (101 MHz, DMSO) δ 166.9, 165.9, 160.8, 159.7, 158.1, 153.0, 150.4, 148.9, 140.3, 130.2, 125.8, 121.3, 121.2, 120.8, 115.5, 114.1, 93.4, 85.9, 55.3, 29.3. HPLC t_R: 11.1 min. MS (ESI+) m/z = 536.93.

4.31. Biology

4.31.1. Chemicals and reagents

[^{3}H]1,3-dipropyl-8-cyclopentyl-xanthine was purchased from ARC Inc. (St. Louis, USA). [^{3}H]ZM241385 was obtained from Tocris Cookson, Ltd. (U.K.). [^{3}H]PSB603 and [^{3}H]PSB11 were obtained from Prof. C. Müller (University of Bonn, Germany). Adenosine deaminase (ADA) was purchased from Boehringer Mannheim (Mannheim, Germany). DPCPX was from Sigma (St. Louis, MO, U.S.A). Bicinchoninic acid (BCA) and BCA protein assay reagent were obtained from Pierce Chemical Company (Rockford, IL, U.S.A.). Chinese hamster ovary cells stably expressing the hA_1R were obtained from Prof. Steve Hill (University of Nottingham, UK). HEK 293 cells stably expressing the human adenosine A_{2A}, A_{2B} and A_3 receptor were gifts from Dr. J. Wang (Biogen, U.S.A.) and Dr. K.-N. Klotz (University of Würzburg, Germany), respectively. All other chemicals were of analytical grade and obtained from standard commercial sources.

4.32. Binding assays

Binding assays were carried out as reported previously [5].

Displacements of radioligands in the presence of 1 μM of unlabeled compounds are an average of at least two independent experiments, each consisting of two replicates. Affinity values are an average of at least three independent experiments, each consisting of two replicates [28].

4.33. Competition association assays

Competition association assays were carried out as reported previously [5].

4.34. Functional assays

[^{35}S]GTPγS binding assay: Membrane homogenates (CHO-hA_1, 3 μg, saponin, 3 μg) were equilibrated in 80 μl total volume of assay buffer (50 mM Tris, 100 mM NaCl, 5 mM $MgCl_2$, pH 7.4, 1 mM EDTA, 1 mM DTT, and 0.05% BSA) containing 3 μM GDP and a range of concentrations of ligand at 25 °C for 30 min. After this 20 μl of [^{35}S]GTPγS (final concentration 0.3 nM) was added and incubation continued for 90 min at 25 °C. The incubation was terminated by filtration over Whatman GF/B filters under reduced pressure with a Brandell harvester or through 96-well GF/B filter plates using a PerkinElmer Filtermate-harvester. Filters were washed three times with ice-cold buffer and placed in scintillation vials. Emulsifier Safe (3.5 mL) was added, and after 2 h radioactivity was counted in an LKB rack β scintillation counter.

4.35. Data analysis

K_i values were calculated by use of a nonlinear regression curve-fitting program (GraphPad Prism 5, GraphPad Software Inc., San Diego, CA). K_D values of the radioligands were 1.6 nM, 1.0 nM, 0.4 nM and 4.9 nM for [^{3}H]DPCPX, [^{3}H]ZM241385, [^{3}H]PSB603 and [^{3}H]PSB11 on the adenosine A_1R, $A_{2A}R$, $A_{2B}R$ and A_3R, respectively. The data from the functional assays were generated and normalized to the value obtained with 100 μM CPA (set at 100%).

4.36. Computational modeling

A homology model of the adenosine A_1 receptor was constructed using the homology modeling tool within the software

package Maestro (version 3.7). [29–31]. The model was based on the active structure of the Adenosine A_{2A} receptor co-crystalized with UK-432097 (PDB: 3QAK) [32]. The alignment between the receptor and templates was performed using ClustalW and GPCRDB for the TM-regions [33]. Based on this alignment a homology model was constructed using the energy-based scoring function. Next, two rounds of ligand-guided optimization were performed [34]. For this we used a set of 76 in house LUF ligands [35]. These ligands were matched with 50 decoys each using the DUD-E web service [36]. In addition to the decoys we added 18 LUF compounds that had been found to be inactive [35]. To ensure proper docking of the LUF ligands and to force a bidentate interaction with $Asn254^{6.55}$, H-bond constraints were used and the VdW radii were lowered to 0.50 Å. After docking 65 models were generated using the top three scoring ligands (LUF7052 [35], **4**, **5**). These ligands were refined using 100 steps of Minimization Monte Carlo present in Prime. [31,32]. Next the best scoring model was selected based on early enrichment (BEDROC-160.9) [37]. We further optimized this model using extended loop sampling on EL3 [31,32] returning a total of 50 models with different conformations. From these models the best performing model showed excellent enrichment (BEDROC-160.9 = 0.844/EF 1% = 48%).

Author information

Notes

The authors declare no competing financial interests.

Author contributions

J.L. conceived the study, A.P.IJ. and L.H.H. supervised the project. The chemical synthesis was designed and supervised by J.L. and performed by M.S. and J.L. The bioassays were supervised by D.G. and J.L. and performed by J.L., T.M.-K. and T.A.M.M. The computational study was performed by E.B.L. The manuscript was written by J.L., E.B.L. and A.P.IJ. All authors have given approval to the final version of the manuscript.

Funding sources

NWO TOP subsidy (714.011.001) to A. P. IJzerman.

Acknowledgment

The authors would like to thank J. P. D. van Veldhoven for carefully reviewing the manuscript.

Appendix A. Supplementary data

Supplementary data related to this article can be found at http://dx.doi.org/10.1016/j.ejmech.2015.07.023.

References

[1] a) B.B. Fredholm, A.P. IJzerman, K.A. Jacobson, J. Linden, C.E. Müller, International Union of basic and clinical pharmacology. LXXXI. Nomenclature and classification of adenosine receptors—an update, Pharmacol. Rev. 63 (2011) 1–34;
b) K.A. Jacobson, Z.G. Gao, Adenosine receptors as therapeutic targets, Nat. Rev. Drug Disc. 5 (2006) 247–264;
c) B.B. Fredholm, J.F. Chen, S.A. Masino, J.M. Vaugeois, Actions of adenosine at its receptors in the CNS: insights from knockouts and drugs, Annu. Rev. Pharmacol. Toxicol. 45 (2005) 385–412.
[2] Bayer Aktiengesellschaft WO2001025210.
[3] a) M.W. Beukers, L.C.W. Chang, J.K. von Frijtag Drabbe Künzel, T. Mulder-Krieger, R.F. Spanjersberg, J. Brussee, A.P. IJzerman, New, non-adenosine, high-potency agonists for the human adenosine A_{2B} receptor with an improved selectivity profile compared to the reference agonist *N*-ethylcarboxamidoadenosine, J. Med. Chem. 47 (2004) 3707–3709;
b) L.C.W. Chang, J.K. von Frijtag Drabbe Künzel, T. Mulder-Krieger, R.F. Spanjersberg, S.F. Roerink, G. van den Hout, M.W. Beukers, J. Brussee, A.P. IJzerman, A series of ligands displaying a remarkable agonistic-antagonistic profile at the adenosine A_1 receptor, J. Med. Chem. 48 (2005) 2045–2053.
[4] a) Otsuka Pharmaceuticals WO2005105778 A2;
b) Otsuka Pharmaceuticals US20120022077 A1.
[5] J. Louvel, D. Guo, M. Agliardi, T.A.M. Mocking, R. Kars, T.P. Pham, L. Xia, H. de Vries, J. Brussee, L.H. Heitman, A.P. IJzerman, Agonists for the adenosine A_1 receptor with tunable residence time. A case for non-ribose 4-amino-6-aryl-5-cyano-2-thiopyrimidines, J. Med. Chem. 57 (2014) 3213–3222.
[6] R.A. Prentis, Y. Lis, S.R. Walker, Pharmaceutical innovation by the seven UK-owned pharmaceutical companies (1964–1985), Br. J. Clin. Pharmacol. 25 (1988) 387–396.
[7] a) D.A. Smith, B.C. Jones, D.K. Walker, Design of drugs involving the concepts and theories of drug metabolism and pharmacokinetics, Med. Res. Rev. 16 (1996) 243–266;
b) R. Zhang, F. Monsma, The importance of drug-target residence time, Curr. Opin. Drug. Disc. Dev. 12 (2009) 488–496;
c) R. Zhang, F. Monsma, Binding kinetics and mechanism of action: toward the discovery and development of better and best in class drugs, Exp. Opin. Drug Disc. 5 (2010) 1023–1029;
d) R.A. Copeland, D.L. Pompliano, T.D. Meek, Drug-target residence time and its implications for lead optimization, Nat. Rev. Drug Discov. 5 (2006) 730–739.
[8] a) M.R. Dowling, S.J. Charlton, Quantifying the association and dissociation rates of unlabelled antagonists at the muscarinic M_3 receptor, Br. J. Pharmacol. 148 (2006) 927–937;
b) I. Van Liefde, G. Vauquelin, Sartan–AT_1 receptor interactions: In vitro evidence for insurmountable antagonism and inverse agonism, Mol. Cell. Endocrinol. 302 (2008) 237–243.
[9] R.A. Copeland, The dynamics of drug-target interactions: drug-target residence time and its impact on efficacy and safety, Exp. Opin. Drug Disc. 5 (2010) 305–310.
[10] Bayer Healthcare Aktiengesellschaft clinical trial report BAY 68-4986/12679.
[11] Bayer Healthcare Aktiengesellschaft WO2007073855 A1.
[12] O. Oniga, I. Grosu, S. Mager, I. Simiti, Heterocycles LXXVIII. Electrophilic substitution of 2′-phenyl-4*R*-2,4′-bisthiazoles, Monatsh. Chem. 129 (1998) 661–669.
[13] M.J. Lohse, K.N. Klotz, J. Lindenborn-Fotinos, M. Reddington, U. Schwabe, R.A. Olsson, 8-Cyclopentyl-1,3-dipropylxanthine (DPCPX) – a selective high affinity antagonist radioligand for A_1 adenosine receptors, Naunyn-Schmiedeberg's Arch. Pharmacol. 336 (1987) 204–210.
[14] D. Guo, E.J. van Dorp, T. Mulder-Krieger, J.P. van Veldhoven, J. Brussee, A.P. IJzerman, L.H. Heitman, Dual-point competition association assay: a fast and high-throughput kinetic screening method for assessing ligand-receptor binding kinetics, J. Biomol. Screen. 18 (2013) 309–320.
[15] R. Wilcken, M.O. Zimmermann, A. Lange, A.C. Joerger, F.M. Boeckler, Principles and applications of halogen bonding in medicinal chemistry and chemical biology, J. Med. Chem. 56 (2013) 1363–1388.
[16] J.J. Dynes, F.L. Baudais, R.K. Boyd, Inter-ring dihedral angles in polychlorinated biphenyls from photoelectron spectroscopy, Can. J. Chem. 63 (1985) 1292–1299.
[17] Ligand efficiencies were calculated using the equation LE (kcal/mol heavy atom) = (1.374/*N*) *p*Ki (at 293 K) clogP values were calculated using Chemaxon Marvin: http://www.chemaxon.com/marvin/sketch/index.jsp.
[18] A.L. Hopkins, C.R. Groom, A. Alex, Ligand efficiency: a useful metric for lead selection, Drug Discov. Today 9 (2004) 430–431.
[19] a) C.A. Lipinski, F. Lombardo, B.W. Dominy, P.J. Freeney, Experimental and computational approaches to estimate solubility and permeability in drug discovery and development settings, Adv. Drug. Deliv. Rev. 23 (1997) 3–25;
b) ibid Adv. Drug. Deliv. Rev. 46 (2001) 3–26.
[20] S.P.H. Alexander, P.J. Millns, [^{3}H]ZM241385–an antagonist for adenosine A_{2A} receptors in rat brain, Eur. J. Pharmacol. 411 (2001) 205–210.
[21] T. Borrmann, S. Hinz, D.C.G. Bertarelli, W. Li, N.C. Florin, A.B. Scheiff, C.E. Müller, 1-alkyl-8-(piperazine-1-sulfonyl)phenylxanthines: development and characterization of adenosine A_{2B} receptor antagonists and a new radioligand with subnanomolar affinity and subtype specificity, J. Med. Chem. 52 (2009) 3994–4006.
[22] C.E. Müller, M. Diekmann, M. Thorand, V. Ozola, [^{3}H]8-Ethyl-4-methyl-2-phenyl-(8*R*)-4,5,7,8-tetrahydro-1H-imidazo[2,1-i]-purin-5-one ([3H]PSB-11), a novel high-affinity antagonist radioligand for human A_3 adenosine receptors, Bioorg. Med. Chem. Lett. 12 (2002) 501–503.
[23] W.H. Moos, D.S. Szotek, R.F. Bruns, N^6-cycloaklyladenosines. Potent, A_1 selective adenosine agonists, J. Med. Chem. 28 (1985) 1383–1384.
[24] J.R. Lane, C. Klein Herenbrink, G.J.P. van Westen, J.A. Spoorendonk, C. Hoffmann, A.P. IJzerman, A novel nonribose agonist, LUF5834, engages residues that are distinct from those of adenosine-like ligands to activate the adenosine A_{2A} receptor, Mol. Pharmacol. 81 (2012) 475–487.
[25] P. Schmidtke, F. Javier Luque, J.B. Murray, X. Barril, Shielded hydrogen bonds as structural determinants of binding kinetics: application in drug design, J. Am. Chem. Soc. 133 (2011) 18903–18910.
[26] P. Auffinger, F.A. Hays, E. Westhoff, P. Shing Ho, Halogen bonds in biological

molecules, Proc. Nat. Acad. Sci. U. S. A. 101 (2004) 16789–16794.
[27] D. Guo, J.M. Hillger, A.P. IJzerman, L.H. Heitman, Drug-target residence time – a case for G protein-coupled receptors, Med. Res. Rev. 34 (2014) 856–892.
[28] T. Borrmann, S. Hinz, D.C.G. Bertarelli, W. Li, N.C. Florin, A.B. Scheiff, C.E. Müller, 1-alkyl-8-(piperazine-1-sulfonyl)phenylxanthines: development and characterization of adenosine A_{2B} receptor antagonists and a new radioligand with subnanomolar affinity and subtype specificity, J. Med. Chem. 52 (2009) 3994–4006.
[29] M.P. Jacobson, D.L. Pincus, C.S. Rapp, T.J. Day, B. Honig, D.E. Shaw, R.A. Friesner, A hierarchical approach to all-atom protein loop prediction, Proteins 55 (2004) 351–367.
[30] M.P. Jacobson, R.A. Friesner, Z. Xiang, B. Honig, On the role of the crystal environment in determining protein side-chain conformations, J. Mol. Biol. 320 (2002) 597–608.
[31] Schrödinger, Release 2014-3: Prime, Version 3.7, Schrödinger, LLC, New York, NY, 2014.
[32] F. Xu, H. Wu, V. Katritch, G.W. Han, K. a. Jacobson, Z.-G. Gao, V. Cherezov, R.C. Stevens, Structure of an agonist-bound human A_{2A} adenosine receptor, Sci. (N.Y.) 332 (2011) 322–327.
[33] V. Isberg, B. Vroling, R. van der Kant, K. Li, G. Vriend, D. Gloriam, GPCRDB: an information system for G protein-coupled receptors, Nucleic Acids Res. 42 (2014) D422–D425.
[34] a) V. Katrich, M. Rueda, R. Abagyan, Ligand-guided receptor optimization, Methods Mol. Biol. 857 (2012) 189–205;
b) V. Katritch, V.-P. Jaakola, J.R. Lane, J. Lin, A.P. IJzerman, M. Yeager, I. Kufareva, R.C. Stevens, R. Abagyan, Structure-based discovery of novel chemotypes for adenosine A_{2A} receptor antagonists, J. Med. Chem. 53 (2010) 1799–1809;
c) V. Katritch, I. Kufareva, R. Abagyan, Structure based prediction of subtype-selectivity for adenosine receptor antagonists, Neuropharmacology 60 (2011) 108–115;
d) P. Kolb, K. Phan, Z.-G. Gao, A.C. Marko, A. Sali, K.A. Jacobson, Limits of ligand selectivity from docking to models: in silico screening for A_1 adenosine receptor antagonists, PLoS ONE 7 (2012) 1–9;
e) I. Kufareva, V. Katritch, Participants of Gpcr dock 2013, S. Grudinin, R.C. Stevens, R. Abagyan, Advances in GPCR modeling evaluated by the GPCR dock 2013 assessment: meeting new challenges, Structure 22 (2014) 1120–1139.
[35] See supplementary information for more details.
[36] M.M. Mysinger, M. Carchia, J.J. Irwin, B.K. Shoichet, Directory of useful decoys, enhanced (DUD-E): better ligands and decoys for better benchmarking, J. Med. Chem. 55 (2012) 6582–6594.
[37] Small-Molecule Drug Discovery Suite 2014-3, Glide, Version 6.4, Schrödinger, LLC, New York, NY, 2014.